

beam (B. C. Barish *et al.*, to be published), but differ by 30% from earlier calibration results using a test calorimeter of substantially smaller cross section [B. C. Barish *et al.*, Nucl. Instrum. Methods **130**, 49 (1975)].

⁵B. Aubert *et al.*, Phys. Rev. Lett. **33**, 984 (1974); A. Benvenuti *et al.*, Phys. Rev. Lett. **36**, 1478 (1976).

⁶M. Holder *et al.*, Phys. Rev. Lett. **39**, 433 (1977). These differences may in part result from acceptance effects not having been taken into account in the latter paper. The data reported here represent $\langle y \rangle$ for the complete phase space.

⁷T. Eichten *et al.*, Phys. Lett. **46B**, 274 (1973); W. G. Scott, Ph.D. thesis, University of Oxford, 1974 (unpublished).

⁸This error does not have an overall 4% systematic normalization uncertainty folded in, since we are making comparisons internal to the same data sample.

⁹B. C. Barish *et al.*, Phys. Rev. Lett. **39**, 741 (1977).

¹⁰See, e.g., M. Barnett and F. Martin, SLAC Report No. SLAC-PUB-1892, 1977 (unpublished); I. Karliner and J. D. Sullivan, University of Illinois Report No. ILL-TH-77-18, 1977 (to be published).

¹¹P. C. Bosetti *et al.*, Phys. Lett. **70B**, 273 (1977).

Origin of Muon-Induced Dimuons and Scale Violations at Small x

K. W. Chen^(a)

Michigan State University, East Lansing, Michigan 48823

and

A. Van Ginneken

Fermi National Accelerator Laboratory, Batavia, Illinois 60510

(Received 27 February 1978)

It is argued that if multimMuon events observed in deep-inelastic muon scattering are manifestations of associated charmed-meson production, then the latter may be responsible for a sizable fraction of observed scaling violations at small values of the scaling variable x .

During the past few years, systematic departures from scaling have been observed both in muon and electron scattering experiments.¹⁻³ With increasing q^2 (square of momentum transfer), the nucleon structure function νW_2 rises at small x and falls at large x ($x \equiv q^2/2M\nu$ with M the nucleon mass and ν the energy of the virtual photon). This pattern of scale violations has been compared with theoretical predictions either phenomenological⁴ or derived from the quark structure of the nucleon.⁵

The production characteristics of dimuons ($\mu N \rightarrow \mu\mu N$) and trimuons ($\mu N \rightarrow \mu\mu\mu N$) observed in 150-GeV deep-inelastic muon-nucleus scattering were described previously.⁶ It was shown that 85% of the observed dimuons were unaccounted for by well-established mechanisms. The total of eight kinematically fully reconstructed trimuons can be divided into five "quiet" (inelasticity $\eta < 0.2$) and three inelastic ($\eta > 0.2$) events. The main trimuon backgrounds are assumed to be direct pair production (electromagnetic tridents) and production of vector mesons, especially ψ because of its large (7%) $\mu\mu$ decay branch. Their total contribution is crudely estimated to

be one trimuon (about 0.75 inelastic and 0.25 elastic events).

Since the experiment is biased towards detecting events at large transverse momentum, an obvious mechanism for producing the extra muons is via associated production and decay of heavy particles. Among many possible muon progenitors, the charm-carrying D meson appears the most likely candidate. The D -meson origin of the muons has already been suggested by several authors^{7,8} along with brief analyses. The motivation of the present work is to study the relation of multimMuons and scaling violation assuming charmed-meson origin of the multimMuons. No further evidence beyond that of earlier studies^{7,8} is presented as to the validity of the D -meson origin hypothesis. In contrast with these earlier studies, trimuons are included in the present analysis, and detection efficiencies are treated more realistically.

For any reasonable model of multimMuon production, the total detection efficiency of the experiment is small. The *rate* of multimMuon production appears to be more sensitive to the model assumed than is the *shape* of various kinematical

distributions. This is also true of the background.⁶ For this reason a careful treatment of detection efficiencies is essential.⁹ Since the scaling violation is most pronounced at small x , a cut of $0.015 < x < 0.075$ has been made. 80% of all dimuons belong to this class as do two of three inelastic trimuons.

The basic model adopted for charmed-meson production is that of Bletzacker and Nieh⁷ (BN). This choice of model is rather arbitrary and is motivated mainly by the fact that BN can readily serve as a way to parametrize D -meson production. Because trimuons are of interest, the BN formula is made to apply to $D\bar{D}$ pairs rather than to single D production. This differs insignificantly from BN except near threshold, while treating the kinematics more accurately. The production cross section is given by

$$\frac{d^3\sigma}{dx dy d^3\vec{p}} = (8\pi\alpha^2 MEq^{-4}) F_{\text{ch}}(x, y) f(\vec{p}), \quad (1)$$

where $y = \nu/E$ with E the incident energy, \vec{p} is the momentum of the $D\bar{D}$ pair, α is the fine-structure constant, and M is the nucleon mass. The structure function $F_{\text{ch}}(x, y)$ is assumed to be

$$F_{\text{ch}}(x, y) = A[q^2/(q^2 + 4M_D^2)][(s - s_0)/s]^3 \times e^{-10x'}[1 + (1 - y)^2], \quad (2)$$

where A is a normalization factor, $M_D = 1.86$ GeV, s is the square of the invariant mass of the virtual-photon-nucleon system, s_0 is the threshold s for $D\bar{D}$ production, and $x' = (q^2 + 4M_D^2)/2M\nu$. The inclusive $D\bar{D}$ momentum distribution is taken to be

$$f(p) = Ne^{-az} \exp(-bp_T^2), \quad (3)$$

where N is a normalization factor, $z = p_z/\nu$ with the longitudinal and p_T the transverse $D\bar{D}$ momentum (as noted above, in BN z and p_T refer to a single D). The parameters a, b are fixed in BN: $a = 3$ and $b = (M_D^2 + 0.03q^2)^{-1}$. In this work the weak q^2 dependence of b is removed and a and b are left free. The invariant mass of the $D\bar{D}$ system is chosen from a theoretical distribution of associated production.¹⁰ The decay of $D\bar{D}$ is assumed to be isotropic in the $D\bar{D}$ rest frame. To study trimuon production the correlation between the two D 's is kept. The D is assumed to decay¹¹ into $K^*\mu\nu$ with a 10% branching ratio.

Characteristics of muon production according to the above model are calculated by a Monte Carlo procedure and the muons are then traced through the apparatus. Multiple scattering, en-

ergy loss, straggling, all relevant detail of target-detector geometry, magnetic fields, scanning criteria, known uncertainties in momentum reconstruction, and the x cut are included. Figure 1 presents a comparison of the calculated p_T' distribution (of the nonleading muon) with experiment. In Fig. 2 the z' distribution is shown where $z' = p_z/\nu$ ($p_z =$ longitudinal momentum of nonleading μ). In both graphs the calculation is normalized to the data. With the exception of a few high- p_T' , high- z' events (they are strongly correlated), agreement is satisfactory.

In both Figs. 1 and 2 the choice of parameters is $a = 1$, $b = 0.25$. Neither distribution is very sensitive to this choice, although small b values are favored by the observed p_T' distribution.¹² Preliminary data from a higher-energy experiment¹³ also support small b by comparing the ratio of dimuons produced at each energy with calculation. This ratio is fairly sensitive to the choice of b (it increases by a factor of 2 from $b = 0.25$ to $b = 3$) and also favors slightly the lower values of a . The calculation predicts a $2\mu/3\mu$ ratio of 25 which is quite insensitive to the parameters and is well above the observed ratio of 10 ± 6 .

By using the observed dimuon rate to normalize BN predictions, an estimate is made of the increment in the structure function, νW_2 . The x cut isolates the small- x region where scaling violation is most prominent. The average q^2 of

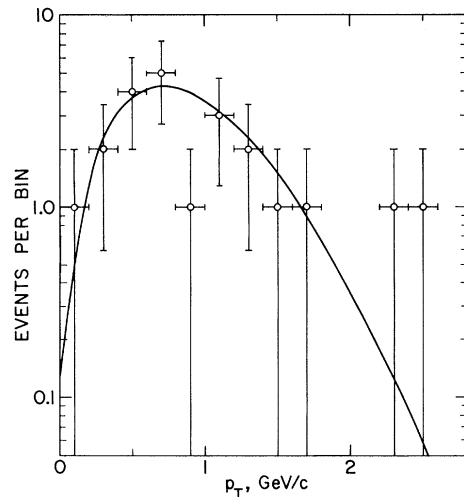


FIG. 1. Transverse-momentum distribution for the produced muon with respect to the virtual-photon direction. The solid curve is the prediction of an associated-charm-production model.

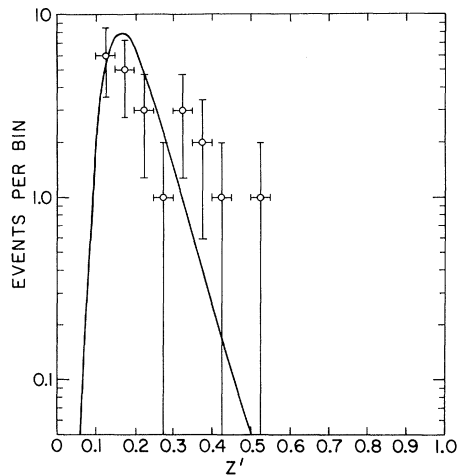


FIG. 2. Distribution of fractional longitudinal momentum, z' . The solid curve is the prediction of an associated-charmed-meson-production model.

the sample is $7.5 \text{ (GeV}/c)^2$. In Fig. 3 the contribution to the scaling violation¹⁴ is plotted as a function of a for values of $b = 0.25$ and $b = 3$. If multimuons are indeed manifestations of charm, one must then conclude that associated charm production is likely a sizable component of the scaling violation at small x .

Other variants of the model are possible,¹⁵ besides those illustrated in Fig. 3. The present analysis concerns only the dominant member of a set of related process, e.g., D decays to different final states such as $K\mu\nu$, $n\pi K\mu\nu$, etc., and associated charmed-meson-baryon production. Based on simple total-cross-section estimates, production of charged or neutral heavy leptons and associated bottom quantum number carriers are not expected to contribute significantly to the multimuon sample of the present experiment.

It is a pleasure to acknowledge useful discussions with E. Lehman and H. T. Nieh. This work was supported in part by the National Science Foundation under Grant No. 6P29070 and by the U. S. Department of Energy.

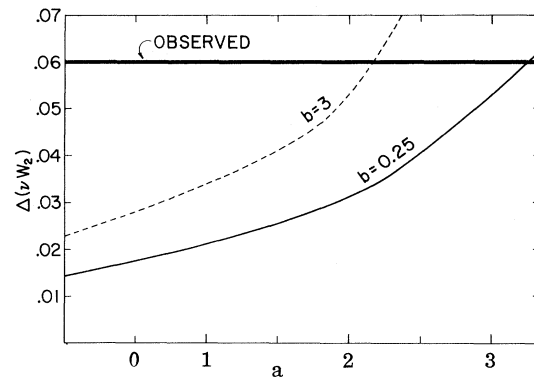


FIG. 3. Average increment in the structure function νW_2 ($0.015 < x < 0.075$) due to associated charm production. The observed scaling violation is shown as a heavy horizontal line. The sensitivity of the parameters used in the model to predict the increment is shown. Small values of a and b appear favored by the analysis.

^{56B}, 36 (1975); I. Karliner and J. D. Sullivan, University of Illinois, Urbana, Report No. ILL-TH-77-18, 1977 (unpublished).

⁵H. D. Politzer, Phys. Rep. 14, 124 (1974), and references therein.

⁶C. Chang, K. W. Chen, and A. Van Ginneken, Phys. Rev. Lett. 39, 519 (1977).

⁷F. Bletzacker, H. T. Nieh, and A. Soni, Phys. Rev. Lett. 37, 1316 (1976); F. Bletzacker and H. T. Nieh, State University of New York at Stony Brook Report No. ITB-SB-77-44, 1977 (unpublished).

⁸E.g., V. Barger and R. J. N. Phillips, Phys. Lett. 65B, 167 (1976); S. Nandi and H. R. Schneider, Phys. Rev. D 15, 3247 (1977); D. P. Roy, Phys. Lett. 69B, 76 (1977); F. Halzen and D. M. Scott, Phys. Lett. 72B, 404 (1978).

⁹Representing the acceptance by a constant energy and constant angle cut ignores the event trigger requirements as well as the strong correlations between the energy and angle cuts.

¹⁰R. Hagedorn and J. Ranft, Nuovo Cimento, Suppl. 6, 169 (1968).

¹¹I. Hinchcliffe and C. H. Llewellyn-Smith, Nucl. Phys. B114, 45 (1976).

¹²The value of $a = 1$ for $D\bar{D}$ production appears in conflict with the observed distribution of light hadrons ($a = 5$); see L. N. Hand, in Proceedings of the International Symposium on Lepton and Photon Interactions at High Energies, Hamburg, Germany, August 1977 (unpublished). This difference can be explained by (a) a dominantly diffractive $D\bar{D}$ production mechanism and (b) the fact that lighter mesons derive preferentially from higher-multiplicity events which tends to concentrate their distribution at smaller values of z' .

¹³K. W. Chen, in Proceedings of the International Symposium on Lepton and Photon Interactions at High Energies, Hamburg, Germany, August, 1977 (unpublished).

^(a)On sabbatical leave at Fermi National Accelerator Laboratory, 1977-1978.

¹C. Chang *et al.*, Phys. Rev. Lett. 35, 1901 (1975).

²E. M. Riordan *et al.*, SLAC Report No. SLAC-PUB-1634, 1975 (unpublished).

³H. Anderson *et al.*, Phys. Rev. Lett. 37, 4 (1976).

⁴E.g., D. Schildknecht and F. Steiner, Phys. Lett.

¹⁴The observed $\Delta(\nu W_2)$ in Fig. 3 is derived by averaging the measure of scaling violations, $(q^2/3)^{(0.25-x)}$, over the dimuon data.

¹⁵For example, the predicted dimuon rate is also somewhat sensitive to the coefficient of x' in the ex-

ponential in (2). Using a value of 8 (also suggested by BN) instead of 10 increases the dimuon rate by about 25% and lowers the predicted scale violation by this same amount. Note also the dependence on the D branching ratio.

Azimuthal Correlations of High-Transverse-Momentum π^0 Pairs

J. H. Cobb, S. Iwata,^(a) R. B. Palmer, D. C. Rahm, R. Rehak, and I. Stumer
Brookhaven National Laboratory, Upton, New York 11973

and

C. W. Fabjan, E. C. Fowler,^(b) I. Mannelli,^(c) P. Mouzourakis, K. Nakamura,^(d) A. Nappi,^(e)
W. Struckzinski,^(e) and W. J. Willis
CERN, Geneva, Switzerland

and

M. Goldberg, N. Horwitz, and G. C. Moneti
Syracuse University, Syracuse, New York 13210

and

C. Kourkouvelis and L. K. Resvanis
University of Athens, Athens, Greece

and

T. A. Filippas
National Technical University, Athens, Greece

and

A. J. Lankford
Yale University, New Haven, Connecticut 06520
(Received 27 December 1978)

We have studied correlations between two π^0 's produced at the CERN intersecting storage rings, utilizing detectors with large azimuthal acceptance. We find that the previously observed enhancement of two π^0 's produced at azimuthal difference near 180° can be made to vanish when certain kinematic effects are removed. However, we observe aligned configurations above 8 GeV of transverse energy unexplained by such kinematic effects.

Most studies¹ of correlations between two particles of high transverse momentum have been limited to nearly coplanar configurations (azimuthal-angle difference $\Delta\varphi \sim 0^\circ$, $\Delta\varphi \sim 180^\circ$). In this experiment, we have measured the distributions of neutral pion pairs over nearly the full angular range of the azimuthal difference. These measurements enable us to remove certain kinematic effects in the analysis of particles emitted in opposite directions at the CERN intersecting storage rings (ISR). We find that the excess in "back-to-back" π^0 pair production previously ob-

served can be made to vanish when these kinematic effects are removed, reappearing only when one of the π^0 's exceeds 4 GeV/c in transverse momentum.

The data for this study were derived primarily from the ISR runs with c.m. energy $\sqrt{s} = 52$ GeV. The integrated luminosity was $\sim 3 \times 10^{36}$ cm⁻². Our apparatus (cf. Kourkouvelis² and Cobb² for a more detailed description) consists of four lead-liquid-argon calorimeters placed adjacently around the intersection region, each covering the polar-angle region $90^\circ \pm 45^\circ$ and each having